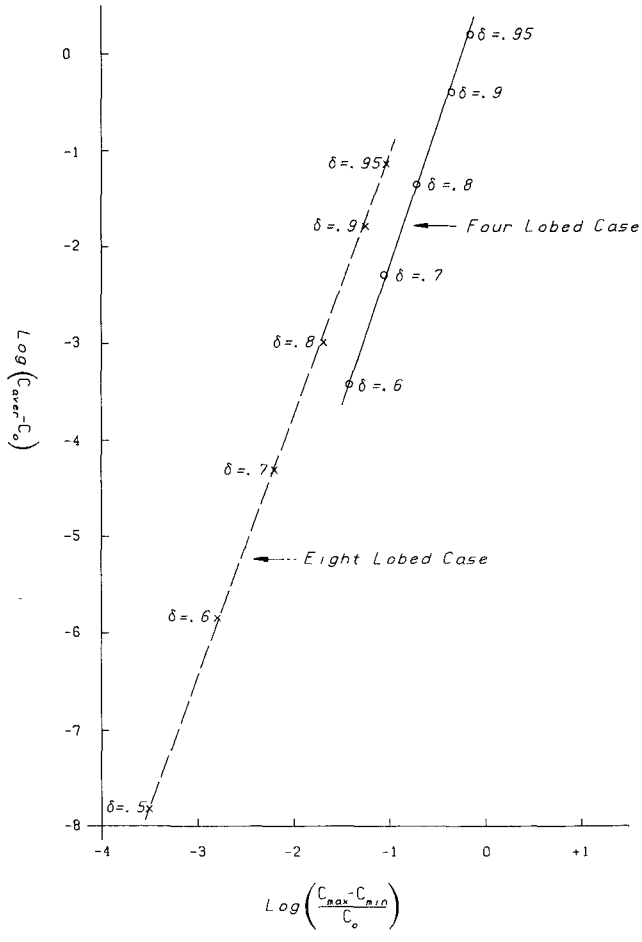

Fig. 4. Comparison of approximation errors.

approximation is about an order of magnitude more accurate than the eight-lobed approximation, but this result is offset by the reduction in the values of the $(C_{\max} - C_{\min})/C_0$ as δ becomes smaller.

V. Comments

It is interesting that both Table I and Table II show that $C_{\text{mean}} - C_0$ becomes positive for sufficiently large values of δ. The fact that the calculation for the four-lobed case involves, at most, the determination of K and K' using the rapidly converging AGM series virtually rules out the possibility of a numerical error. The computation for the eight-lobed case is more involved, but here great care was taken to check the accuracy of each step in the calculations. For example, each complex value of w obtained by applying the Gauss descending transformation to the given v and k was checked for accuracy by resubstituting into $v = \text{sn}(w, k)$. It is believed that these results are accurate to the order of 10^{-9}.

In both cases, it will be observed that the geometric mean of $C_{\max}$ and $C_{\min}$ is a more accurate approximation than their average. It was only because the error in the average of $C_{\max}$ and $C_{\min}$ changes sign for smaller values of δ, however, that the logarithm of the error in the average is plotted in Fig. 4. Needless to say, the linearity of the data for the two cases and their parallelism were a surprise.

References

[1] F. Oberhettinger and W. Magnus, *Anwendung der Elliptischen Funktionen in Physik and Technik*. Berlin, Germany: Springer, 1949.

[2] P. A. A. Laura and L. E. Luisoni, "Approximate determination of the characteristic impedance of the coaxial system consisting of a regular polygon concentric with a circle," *IEEE Trans. Microwave Theory Tech.*, vol. MTT-25, pp. 160–161, Feb. 1977.

[3] H. J. Riblet, "Expansions for the capacitance of a cross concentric with a circle with an application," *IEEE Trans. Microwave Theory Tech.*, vol. 37, Nov. 1989.

[4] H. J. Riblet, "Expansions for the capacitance of a cross concentric with a square with an identity," *IEEE Trans. Microwave Theory Tech.*, vol. 38, Oct. 1990.

[5] F. Bowman, *Introduction to Elliptic Functions with Applications*. New York: Dover Publications, 1961.

[6] Arthur Cayley, *Elliptic Functions*. New York: Dover Publications, 1961.

A New Procedure for Interfacing the Transmission Line Matrix (TLM) Method with Frequency-Domain Solutions

Zhizhang Chen, Wolfgang J. R. Hoefer, and Michel M. Ney

Abstract—**This paper presents a new procedure that interfaces the transmission-line matrix method (TLM) with frequency-domain solutions of electromagnetic fields. Frequency-domain solutions are transformed into appropriate time-domain sequences using the discrete Fourier transform (DFT). Hence, the corresponding boundary Johns matrix can be determined with minimum computational effort. The subsequent treatment consists in convolving the streams of TLM impulses incident on the boundary with a Johns matrix generated with the new approach. The method is applied to obtain the time-domain reflection sequence of wide-band absorbing terminations in a rectangular waveguide in the dominant mode operation. In addition, the time-domain analysis of pulse penetration through a sheet with high, but finite, conductivity is presented. Good results demonstrate the efficiency of the proposed procedure.**

I. Introduction

The transmission line matrix (TLM) method has been extensively applied to solve electromagnetic wave propagation, diffusion, and network problems in the time domain [1]–[3]. With its flexibility and the simplicity of the basic algorithm, the TLM method can handle arbitrary geometries and account for realistic features that are often neglected with other methods. Recently, two- and three-dimensional transmission line matrix microwave field simulators using new concepts and procedures have been presented [4].

In order to characterize structures with large dimensions, the TLM technique requires large memory space and CPU time. More recently, a general partitioning technique based on the Johns matrix concept [5], [6] has been developed to overcome this problem for certain applications.

In the following, a new procedure for interfacing TLM techniques with frequency-domain solutions is described: either scat-

Manuscript received November 7, 1990; revised March 14, 1991.

The authors are with the Department of Electrical Engineering, University of Ottawa, Ottawa, Canada K1N 6N5.

IEEE Log Number 9102334.

tering parameters or the relations between electric and magnetic fields on a boundary or interface limiting regions, computed in the frequency domain, are transformed into time-domain sequences. The sequences of impulses are equivalent to the ones that would produce a corresponding Johns matrix, describing subregions for TLM simulations [7]. The subsequent step is to convolve any impulse stream incident upon such a boundary with the time-domain sequences or Johns matrix thereby generated.

II. Basic Theory

Let $X(f)$ be a frequency-domain solution, for example, a frequency-dependent complex reflection coefficient, and $x(t)$ the corresponding time-domain solution. Then by sampling or discretizing $X(f)$, one can obtain the corresponding discrete $x(t)$ via various synthesis techniques. For the sake of simplicity, the discrete Fourier transform (DFT) technique is employed in this paper.

The discrete and inverse discrete Fourier transforms are [8]

$$X_k = \sum_{i=0}^{N-1} x_i e^{jik(2\pi/N)}, \qquad k = 0,1,2,\cdots,N-1 \quad (1)$$

$$x_k = \frac{1}{N} \sum_{i=0}^{N-1} X_i e^{-jik(2\pi/N)}, \qquad k = 0,1,2,\cdots,N-1 \quad (2)$$

where

$$X_k = X(k\Delta f) \quad (3)$$

$$x_k = x(k\Delta t) = \frac{1}{N} \sum_{i=0}^{N-1} X_i e^{-jik(2\pi/N)} \quad (4)$$

and j is the complex operator ($j = \sqrt{-1}$), N is the total number of iterations of the time-domain solution or the total number of sampling points of the frequency-domain solution, $\Delta f = 1/(N\Delta t)$ is the sampling frequency, and Δt is the time step determined by the TLM model.

TLM simulations require that any time-domain solution be real. Therefore, in order to make x_k compatible with the TLM, x_k must be real. As a result, X_k must satisfy the following conditions [8]:

$$\mathrm{Re}(X_{N-k}) = \mathrm{Re}(X_k) \quad (5)$$

$$\mathrm{Im}(X_{N-k}) = -\mathrm{Im}(X_k) \quad (6)$$

where $k = 1,2,\cdots,(N/2)-1$ when N is even and $k = 1,2,\cdots,(N-1)/2$ when N is odd. Consequently, before computing $x(k\Delta t)$ from $X(k\Delta f)$ via (4), one should modify $X(f)$ or $X(k\Delta f)$ so that (5) and (6) are satisfied. As shown in Fig. 1 the modified $X(f)$ or $X(k\Delta f)$ are the same as the original $X(f)$ or $X(k\Delta f)$ at least for $f \leqslant \left(\frac{N}{2} - 1\right)\Delta f$ when N is even, or $f \leqslant \frac{N-1}{2}\Delta f$ when N is odd. On the other hand, as indicated in [3], the dispersion caused by the space and time discretization of TLM networks can be neglected only when the operating frequency, f, is below a certain value, say $f_{\max}$. For example, in 2-D shunt node TLM models, one may select $\Delta l/\lambda \leqslant 0.1$ or $f \leqslant f_{\max} = 0.1c/\Delta l$ (c the speed of light) as the practically dispersionless frequency range in free space (0.1 factor can be smaller, depending on the required minimum dispersion error). This means that the TLM solution can only be accurate for

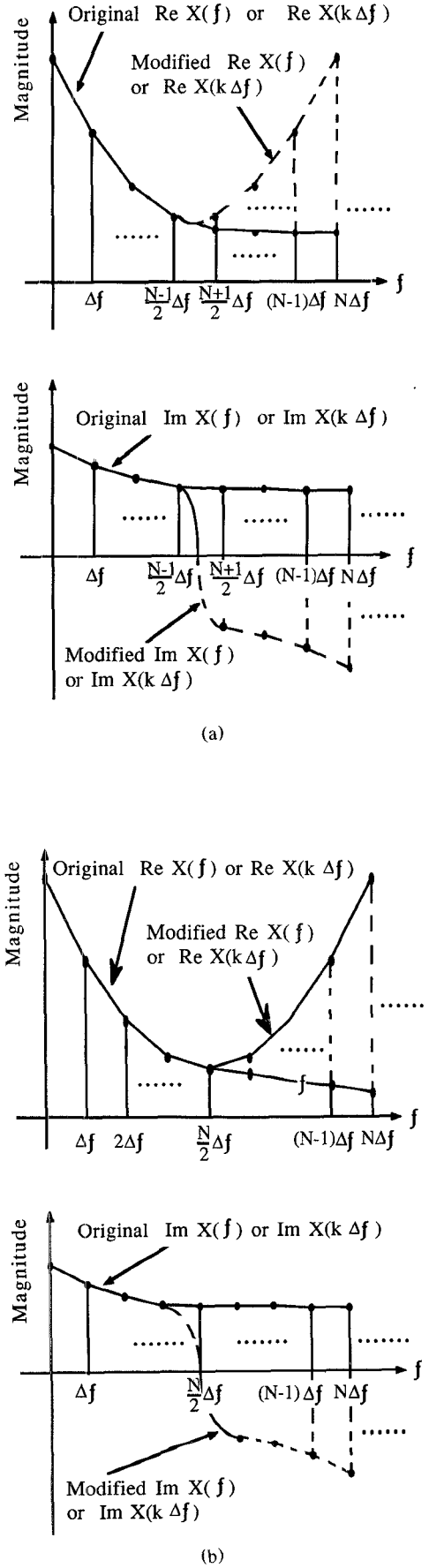

Fig. 1. (a) The original and the modified $X(f)$ or $X(k\Delta f)$ for N odd. (b) The original and the modified $X(f)$ or $X(k\Delta f)$ for N even.

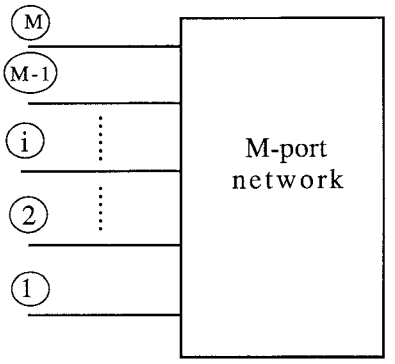

Fig. 2. M-port microwave network.

$f \leqslant f_{\max}$. Thus, N or Δf should be chosen in such a way that

$$\left(\frac{N}{2}-1\right)\Delta f \geqslant f_{\max} \qquad \text{for } N \text{ even} \tag{7}$$

$$\left(\frac{N-1}{2}-1\right)\Delta f \geqslant f_{\max} \qquad \text{for } N \text{ odd.} \tag{8}$$

This ensures that the frequency at which the discrete spectrum is modified to satisfy conditions (5) and (6) is beyond the frequency limit at which the TLM solution is accurate. In addition, one can use a low-pass digital filter in order to reject the unwanted high-frequency components of the time-domain sequence x_k before it can be convolved with the incident sequence. This is simply achieved by doing the convolution of the x'_ks with the noncausal discrete impulse response of the appropriate low-pass filter.

III. Johns Matrix Generation of a Microwave Network

Consider an M-port network, as shown in Fig. 2, with its given frequency-domain scattering parameters $[S(f)]$. If the scattering parameters are defined with respect to field quantities and, therefore, are compatible with the TLM quantities, the Johns matrix can be obtained from (3) and (4):

$$G(n,m,k)=\frac{1}{N}\sum_{i=0}^{N-1} S_{nm}(i\Delta f)e^{-j\imath k\Delta f} \tag{9}$$

where $m,n=1,2,\cdots,M,N$ are the numbers of iterations, and $\Delta f=1/(N\Delta t)$ is the sampling frequency. In addition, according to (5) and (6), $S_{nm}(f)$ must be modified so that

$$\operatorname{Re} S_{nm}((N-i)\Delta f)=\operatorname{Re} S_{nm}(i\Delta f) \tag{10}$$

$$\operatorname{Im} S_{nm}((N-i)\Delta f)=-\operatorname{Im} S_{nm}(i\Delta f). \tag{11}$$

Finally, the output sequence of $V^r(n,k)$ at port n is obtained by convolution of the Johns matrix, generated via (9), with the incident impulses at every port:

$$V^r(n,k)=\sum_{m=1}^{M}\sum_{k'=0}^{K} G(n,m,k-k')V^i(m,k'). \tag{12}$$

Once the Johns matrices of several networks are known, the cascading of the networks in the time domain can be performed using Bewley diagram, which is described in detail by Hoefer [7].

The method described here saves considerable computation time and memory for generating the Johns matrix, especially when the frequency-domain scattering parameters $S(f)$ of the network at the sampling points $k\Delta f$ can be expressed analytically or obtained by measurements. The principle of the method is general and can be easily extended to a variety of electromagnetic problems such as three-dimensional inhomogeneously filled and unbounded structures.

IV. Numerical Results

A. Application to Wide-Band Absorbing Boundaries in Waveguides

Owing to finite computer resources, the TLM mesh must be limited at some locations where appropriate boundary conditions, such as absorbing boundaries or matched loads, are inserted in order to simulate the properties of the truncated region. The methods for obtaining TLM wide-band absorbing boundaries in waveguides were recently described in a paper by Eswarappa *et al.* [9]. Two different approaches were employed:

a) modeling of a waveguide termination with gradually increasing loss,
b) modeling of a waveguide termination with a very long uniform waveguide section.

With the method presented in this paper, instead of modeling the termination physically by waveguide sections, the TLM absorbing boundary termination or matching load of the waveguide is modeled by an artificially reflecting wall with the frequency-domain reflection coefficient $\Gamma(f)$:

$$\Gamma(f)=\frac{Z(f)/\sqrt{2}-\eta_0}{Z(f)/\sqrt{2}+\eta_0} \tag{13}$$

where $Z(f)=\eta_0/\sqrt{\epsilon_r-(f_c/f)^2}$ is the wave impedance of the dominant mode in the waveguide, f is the operating frequency, f_c is the cutoff frequency of the air-filled waveguide, ϵ_r is the relative permittivity of the medium filling the guide, η_0 is the characteristic impedance of the link line of the TLM network, and the correction factor $\sqrt{2}$ is inherent to the slow-wave property of the 2-D TLM network [3].

Now, the procedure outlined in this paper is applied to the case of a WR28 waveguide. A section of it with a width of $30\Delta l$ is terminated at each side by absorbing boundaries (or matched load) for the dominant mode (see Fig. 3(a)). First, a time-domain sequence is generated by computing the inverse DFT of (13), corresponding to both limiting absorbing boundaries. The CPU time required for generating the sequences is only few seconds, which is at least three orders of magnitude below that reported in [9] if those approaches are used to obtain the same time-domain sequences. Subsequently, a TE_{10} mode field is injected in the TLM mesh with impulse time function, in order to simulate a wide-band excitation. As the TLM impulses propagate through the TLM network and reach the absorbing boundaries, they are convolved at the boundary nodes with the stored sequences simulating the absorbing boundaries. After a sufficient number of iterations (in this case 2000), the Fourier transform of the signal is performed at a few nodes (a minimum of two is required), from which the VSWR can be easily and rapidly determined and, therefore, the return loss calculated. Fig. 3(b) shows the return loss produced by both terminations over a wide frequency range. One can see that a return loss better than -35 dB is achieved over the operating range.

B. Application to Highly Conductive Shields

The method can also be applied to the case of electromagnetic field diffusion through highly conducting materials. A typical application is the evaluation of shield effectiveness of

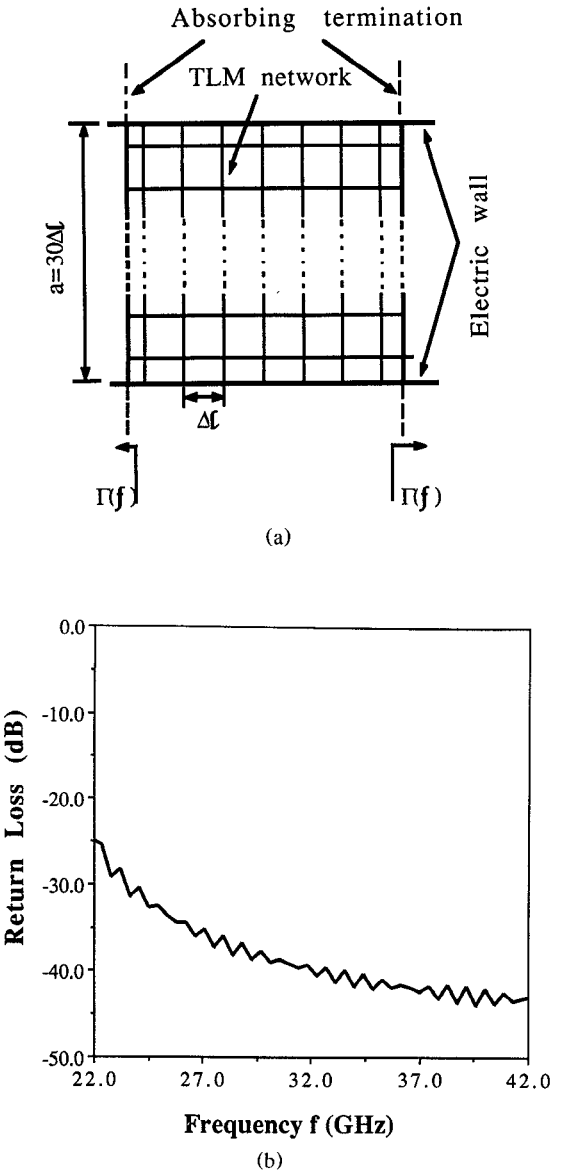

Fig. 3. (a) TLM model for a WR28 rectangular waveguide. (b) Return loss of two back-to-back absorbing terminations for WR28. The ripple indicates mismatch at high frequencies caused by discretization.

cavities against electromagnetic interference (EMI). The excitation is most likely a transient function, for which a time-domain solution is the most appropriate. The TLM is an ideal tool for that application, except that in order to avoid network space and frequency dispersion, a very large number of nodes are necessary within highly conducting media [3] because of high conductivity, making the computational effort beyond practical limit.

In order to circumvent this problem, a Johns matrix can be used. Unfortunately, for the reasons explained above, the generation of such a matrix requires a large amount of CPU time and memory core in most practical cases. However, with the method described here, the shielding wall can be replaced by a section of lossy transmission line inserted into the TLM network as shown in Fig. 4. It is assumed that adjacent nodes on the conducting surface do not interact, which is a realistic hypothesis if one considers that fields are rapidly attenuated within the shield. The scattering parameters of such lossy lines defined by the electromagnetic field component ratios can be determined

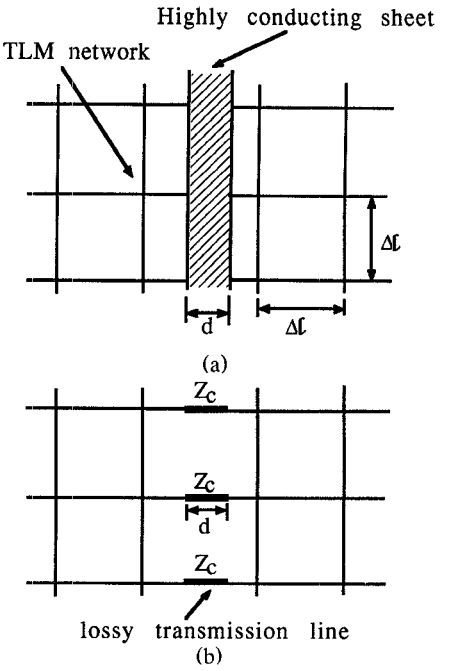

Fig. 4. (a) A TLM network containing a highly conducting sheet. (b) Equivalent TLM network for (a).

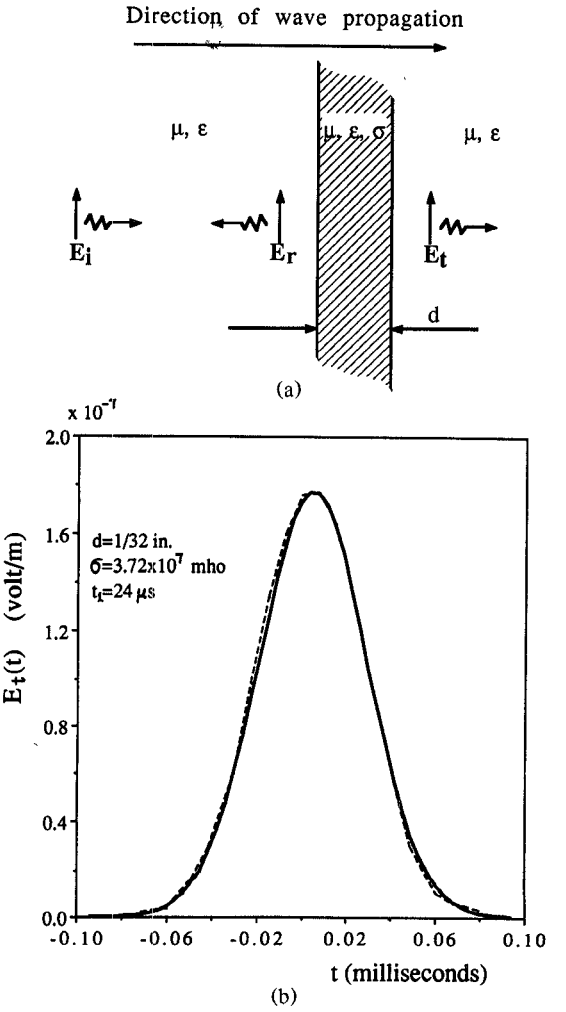

Fig. 5. (a) Infinite conducting sheet with thickness d and conductivity σ. (b) Transient electric field $E_t(t)$ on the far side of the conducting sheet: ---- Harrison's result; —— present method.

easily from a harmonic field analysis or transmission line theory:

$$S_{11} = \frac{Z_1 - 1}{Z_1 + 1} \tag{14}$$

$$S_{12} = \frac{1 + \Gamma_2}{1 + \Gamma_2 e^{-\gamma d}} e^{-2\gamma d}(1 + S_{11}) \tag{15}$$

$$S_{21} = S_{12} \tag{16}$$

$$S_{22} = S_{11} \tag{17}$$

where $\gamma = \sqrt{j\omega\mu(\sqrt{2}\sigma + 2j\omega\epsilon)}$, $Z_c = (2\epsilon_r + (\sqrt{2}\sigma)/j\omega\epsilon_0))^{-1/2}$, $Z_1 = Z_c(1 + Z_c th(\gamma d))/(Z_c + th(\gamma d))$, $\Gamma_2 = (1 - Z_c)/(1 + Z_c)$, $\omega = 2\pi f$, $\epsilon = \epsilon_r \epsilon_0$, f is the frequency, ϵ_0 is the permittivity of the vacuum, and ϵ_r, μ, σ, and d are, respectively, the relative permittivity, permeability, and thickness of the conducting shield. And the correction factor 2 and $\sqrt{2}$ is inherent to the slow-wave property of the 2-D TLM network [3].

The transient field that impinges on a plane conducting wall is modeled by the following time function:

$$e_0(t) = Ae^{-t^2/2t_1^2} \tag{18}$$

where A is the value of $e_0(0)$, t is the time, and t_1 is a measure of the pulse width. A plane wave with the above time dependence was incident on the conducting wall (see Fig. 5(a)). The time function was observed at a node located behind the wall after 1000 iterations. The signal is shown in Fig. 5(b) and compared with an analytical approach whose time-domain solution is found by the numerical inverse Fourier transform calculation [10]. Good agreement between two methods can be observed.

V. Conclusion

A novel procedure based on time–frequency transformation for interfacing TLM algorithm with frequency-domain solutions has been presented. It uses the a priori knowledge of the frequency behavior of such parameters as reflection coefficients, network parameters, and impedances, which are known in many practical situations. The relationship between the frequency-domain parameters and the corresponding Johns matrix of the network based on a DFT has been presented in detail. The examples pertaining to modeling of the absorbing waveguide termination and the field penetration through a highly conductive sheet demonstrate the efficiency of the approach. With respect to CPU time, the procedure for generating the Johns matrix pertaining to such problems is orders of magnitude less than that required by other methods.

References

[1] P. B. Johns and R. L. Beurle, "Numerical solution of 2-dimensional scattering problems using a transmission-line matrix," *Proc. Inst. Elec. Eng.*, vol. 118, no. 9, pp. 1203–1208, Sept. 1971.

[2] W. J. R. Hoefer, "The transmission-line matrix method-theory and application," *IEEE Trans. Microwave Theory Tech.*, vol. MTT-33, pp. 882–893, Oct. 1985.

[3] W. J. R. Hoefer, "The transmission line matrix (TLM) method," in *Numerical Techniques for Passive Microwave and Millimeter-Wave Structures*, T. Itoh, Ed. New York: Wiley, 1989, ch. 8, pp. 486–591.

[4] P. So, Eswarappa, and W. J. R. Hoefer, "A two-dimensional TLM microwave field simulator using new concepts and procedures," *IEEE Trans. Microwave Theory Tech.*, vol. 37, pp. 1877–1883, Dec. 1989.

[5] P. B. Johns and S. Akhtarzad, "The use of time domain diakoptics in time discrete models of fields," *Int. J. Numer. Methods Eng.*, vol. 18, pp. 1361–1373, 1982.

[6] Eswarappa and W. J. R. Hoefer, "Application of time domain diakoptics to 3-D TLM method with symmetrical condensed nodes," presented at 1990 IEEE-AP Symp. and URSI Meeting, Dallas, TX, May 7–11, 1990.

[7] W. J. R. Hoefer, "The discrete time domain Green's function or Johns matrix—A new powerful concept in transmission line modelling," *Int. J. Numer. Modelling: Electronic Networks, Devices and Fields*, vol. 2, no. 4, pp. 215–225, 1990.

[8] V. Cizek, *Discrete Fourier Transforms and Their Applications*. Bristol: Hilger, 1986.

[9] Eswarappa, G. I. Costache and W. J. R. Hoefer, "TLM modelling of dispersive wideband absorbing boundaries with time domain diakoptics for *S*-parameters extraction," *IEEE Trans. Microwave Theory Tech.*, vol. 38, Apr. 1990.

[10] C. W. Harrison, Jr., "Transient electromagnetic field propagation through infinite sheets, into spherical shells, and into hollow cylinders," *IEEE Trans. Antennas Propagat.*, vol. AP-12, pp. 319–334, May 1964.

Open Resonator for Precision Dielectric Measurements in the 100 GHz Band

B. Komiyama, M. Kiyokawa, and T. Matsui

Abstract—**Dielectric properties of fused silica, MgO, AlN, and BN were measured using an open resonator at frequencies around 100 GHz. The resonator is of the semiconfocal type and consists of a concave and a plane mirror, and the frequency variation method is used. To increase the reliability of measurement data, the operating frequency and thickness of the samples were chosen so as to make the parameter $\Delta = 1$ for every sample. The radius of curvature of the concave mirror is deduced with sufficient accuracy from the resonant frequencies of the $TEM_{0,0}$ and $TEM_{1,0}$ modes, which results in a precise determination of resonator length. The standard deviation of measurements was less than 0.1% in permittivity and about 10% in loss tangent.**

I. Introduction

Low-loss dielectric materials are of key importance in short-millimeter-wave circuit components and quasi-optical elements such as windows, lenses, beam splitters, and substrates. With increasing demands for improved performance in these components and elements, the measurement of the properties of dielectric materials in this wave band has become more important [1].

In the short-millimeter-wave region, dispersive Fourier transform spectrometers and interferometric spectrometers of the Mach–Zender type are often used for dielectric measurement [1]–[3]. In comparison with these spectrometers, the Fabry–Perot open resonator technique [4] is more advantageous for the measurement of low-loss materials. However, few data were available at frequencies higher than 35 GHz [5], [6] because of the difficulty in constructing high-Q cavities and detecting absorption with enough S/N at these frequencies.

Manuscript received January 7, 1991; revised April 29, 1991. This work was supported by the Science and Technology Agency.

The authors are with the Communications Research Laboratory, 4-2-1 Nukui-Kita Koganei, Tokyo 184, Japan.

IEEE Log Number 9102331.